PERGAMON

International Journal of Solids and Structures 37 (2000) 7689–7702

INTERNATIONAL JOURNAL OF SOLIDS and STRUCTURES

www.elsevier.com/locate/ijsolstr

Elasticity solutions for free vibrations of annular plates from three-dimensional analysis

K.M. Liew [a,*,1], B. Yang [b]

[a] *Centre for Advanced Numerical Engineering Simulations, School of Mechanical and Production Engineering, Nanyang Technological University, Nanyang Avenue, Singapore 639798*

[b] *Department of Mechanical Engineering, University of Southern California, Los Angeles, CA 90089-1453, USA*

Received 30 May 1998

Abstract

This article, examines the vibrational characteristics of annular plates by using the three-dimensional elasticity theory. It aims to raise the quality of the investigation beyond that provided by the two-dimensional plate theories by resorting to a full three-dimensional analysis. A polynomials–Ritz model based on sets of orthogonally generated polynomial functions to approximate the spatial displacements of the plates in cylindrical polar coordinates is presented. The model is then used to extract the full vibration spectrum of natural frequencies and mode shapes. The vibration responses due to the variations of boundary conditions and thickness are investigated. Frequency parameters and three-dimensional deformed mode shapes are presented in vivid graphical forms. The accuracy of the method is validated through appropriate convergence and comparison studies. © 2000 Published by Elsevier Science Ltd.

Keywords: Annular plates; Frequency; Mode shape; Polynomials; Ritz method; Three-dimensional elasticity; Vibration

1. Introduction

Plates are customarily used as structural components in various engineering applications. They can be analysed based on two-dimensional theories, such as the classical plate theory (CPT), the first-order shear deformable plate theory, and the higher-order shear deformable plate theory (Liew et al., 1995a). Although adequate for many engineering applications for sufficiently thin plates, much of what has been done in free vibration analysis of annular plates based on the CPT has certain limitations due to the Kirchhoff hypothesis (Leissa, 1969; Kim and Dickinson, 1989; Liew, 1993). The CPT neglects the effects of transverse shear deformation and rotary inertia, leading to overestimation of the vibration frequencies. The error increases with increasing plate thickness. To refine CPT by including the shear effect in the analysis of thick plates, various shear deformation theories have been proposed during the past few decades. The first paper

* Corresponding author. Fax: +65-793-6763.

E-mail address: mkmliew@ntu.edu.sg (K.M. Liew).

[1] This work was carried out during the author's sabbatical as visiting professor at the University of Southern California.

0020-7683/00/$ - see front matter © 2000 Published by Elsevier Science Ltd.
PII: S0020-7683(99)00306-6

that appeared in the literature for free vibration analysis of circular plates with the inclusion of shear and rotary inertia effects was due to Deresiewicz and Mindlin (1955). This work was further extended by Irie et al. (1982) for annular Mindlin plates with nine different combinations of free, simply supported and clamped boundary conditions. Vibration analysis of annular Mindlin plates continuous over multiple internal ring supports was recently considered by Liew et al. (1993a).

The two-dimensional theories offer a relatively simple mathematical manipulation in analytical or computational implementations (Nosier et al., 1993). They reduce the dimensions of the plate problem (and thus the determinant size of the eigenvalue equation) from three to two by addressing the quantities of interest, such as membrane forces, bending moments and shear forces, in terms of certain averages over the displacement across the smaller dimension, i.e., the thickness. These simplifications are inherently erroneous, and therefore may lead to unreliable results for relatively thick plates. Srinivas and Rao (1970) pointed out that the Mindlin plate theory fails to predict a full vibration spectrum for a much thicker simply supported rectangular plate. A similar conclusion was also drawn for thick rectangular plates with other combinations of boundary conditions (Liew et al., 1993b).

The available three-dimensional elasticity solutions for free vibrations of plates are very limited. Three-dimensional elasticity solutions are important because they form a real basis for assessing the results of the two-dimensional theories. Publications on three-dimensional vibration of annular plates, if available, are very limited. This apparent void has thus formed the motivation of the present work. To obtain the solutions for this problem, two computational models could be developed. The first model can be formulated in a Cartesian coordinate system that allows the geometry to be described in a cylindrical coordinate system (Liew and Hung, 1995; Liew et al., 1995b). The second model can be developed based on the cylindrical polar coordinate system. It is expedient to use cylindrical polar coordinates when dealing with annular plates with three-dimensional flexibility. Therefore, in this paper, we adopt the cylindrical polar coordinate system to derive a three-dimensional model (Liew and Yang, 1999), which is applicable to annular plates with different combinations of inner and outer edge boundary conditions.

This article is organized as follows: Section 2 outlines the formulations of the plate strain and kinetic energies in the cylindrical polar coordinate system and the solution method using orthogonal polynomials. Section 3 presents the results of several plate problems obtained from the proposed method, and also the convergence and comparison studies. Section 4 concludes the present investigation.

2. Mathematical formulation

The geometric configuration of a homogeneous isotropic annular plate of constant thickness h is depicted in Fig. 1. The plate geometry and dimensions are defined by a cylindrical polar coordinate system (r, θ, z). The corresponding displacement components at a generic point are u_1, u_2 and u_3 in the radial, circumferential and thickness directions, respectively. The plate inner and outer radii are denoted by r_i and r_o. The natural frequencies and mode shapes of this plate are to be determined from a Ritz three-dimensional displacement-based polynomials method.

2.1. Elastic strain and kinetic energy expressions

The linear elastic strain energy component $\boldsymbol{V}$ for a plate in cylindrical polar coordinates can be written in an integral form as

$$\boldsymbol{V} = \frac{E}{2(1+v)(1-2v)} \int_{r_i}^{r_o} \int_0^{2\pi} \int_{-h/2}^{h/2} \left[\mathbf{A}_1^2 + (1-2v)\left(\mathbf{A}_2 + \frac{1}{2}\mathbf{A}_3 \right) \right] r \, \mathrm{d}r \, \mathrm{d}\theta \, \mathrm{d}z, \tag{1}$$

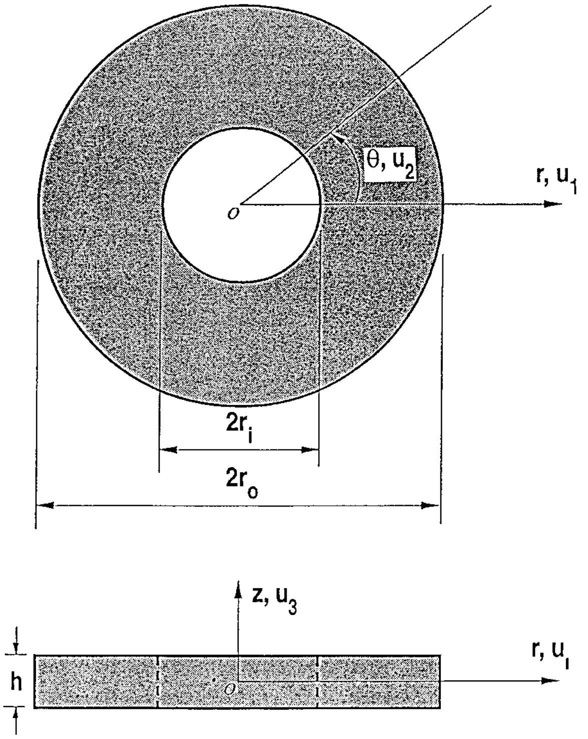

Fig. 1. Geometry and dimensions of an annular plate in cylindrical coordinate system.

where

$$\mathbf{A}_1 = \varepsilon_{rr} + \varepsilon_{\theta\theta} + \varepsilon_{zz}, \tag{2}$$

$$\mathbf{A}_2 = \varepsilon_{rr}^2 + \varepsilon_{\theta\theta}^2 + \varepsilon_{zz}^2, \tag{3}$$

$$\mathbf{A}_3 = \varepsilon_{r\theta}^2 + \varepsilon_{rz}^2 + \varepsilon_{\theta z}^2. \tag{4}$$

E is the Young's modulus, v, the Poisson ratio, and the strain components in cylindrical polar coordinate for small deformation are given as

$$\varepsilon_{rr} = \frac{\partial u_1}{\partial r}; \quad \varepsilon_{\theta\theta} = \frac{u_1}{r} + \frac{\partial u_2}{r\partial\theta}; \quad \varepsilon_{zz} = \frac{\partial u_3}{\partial z}, \tag{5}$$

$$\varepsilon_{r\theta} = \frac{\partial u_1}{r\partial\theta} + \frac{\partial u_2}{\partial r} - \frac{u_2}{r}; \quad \varepsilon_{rz} = \frac{\partial u_1}{\partial z} + \frac{\partial u_3}{\partial r}, \tag{6}$$

$$\varepsilon_{\theta z} = \frac{\partial u_2}{\partial z} + \frac{\partial u_3}{r\partial\theta}. \tag{7}$$

For free vibration analysis, the kinetic energy can be expressed as

$$\boldsymbol{T} = \frac{\rho}{2}\int_{r_i}^{r_o}\int_0^{2\pi}\int_{-h/2}^{h/2}\left[\left(\frac{\partial u_1}{\partial t}\right)^2 + \left(\frac{\partial u_2}{\partial t}\right)^2 + \left(\frac{\partial u_3}{\partial t}\right)^2\right] r\,\mathrm{d}r\,\mathrm{d}\theta\,\mathrm{d}z, \tag{8}$$

where ρ is the mass density per unit volume.

For linear small-strain simple harmonic motion, the displacement components assume the following forms:

$$u_\alpha(r,\theta,z,t) = U_\alpha(r,\theta,z)\,\mathrm{e}^{\mathrm{i}\omega t}, \quad \alpha = 1,\ 2,\ 3, \tag{9}$$

where ω denotes the frequency of vibration.

For simplicity and convenience in the mathematical formulation, the cylindrical polar coordinates (r,θ,z) are transformed to a set of nondimensional parameters $(\bar{x}_1,\bar{x}_2,\bar{x}_3)$ by the following relations:

$$\bar{x}_1 = \frac{r}{r_\mathrm{o}}, \quad \bar{x}_2 = \theta, \quad \bar{x}_3 = \frac{z}{h}. \tag{10}$$

The displacement amplitude functions, $U_\alpha(r,\theta,z);\ \alpha = 1,\ 2,\ 3$, are expanded into Fourier components in terms of the circumferential coordinate

$$U_\alpha(\bar{x}_1,\bar{x}_2,\bar{x}_3) = \sum_{m=1}^{M}\sum_{n=1}^{N} C^\alpha_{mn}\phi^\alpha_m(\bar{x}_1)\psi^\alpha_n(\bar{x}_3)\vartheta^\alpha(\bar{x}_2) \quad \alpha = 1,\ 2,\ 3 \tag{11}$$

in which C^α_{mn} are the unknown coefficients, and $\phi^\alpha_m(\bar{x}_1)$ and $\psi^\alpha_n(\bar{x}_3)$ are the one-dimensional polynomials approximating the radial and thickness variations of each displacement component in cylindrical coordinates. In Eq. (11), the function $\vartheta^\alpha(\bar{x}_2)$ is given by

$$\vartheta^\alpha(\bar{x}_2) = \begin{cases} \sin(\bar{n}\bar{x}_2) & \text{if } \alpha = 2, \\ \cos(\bar{n}\bar{x}_2) & \text{if } \alpha = 1 \text{ and } 3\ . \end{cases} \tag{12}$$

The variable $\bar{n}$ in the above expression denotes the number of circumferential nodal diameters in the vibration mode. The following relations are used for evaluating the energy expressions of the annular plate:

$$\int_0^{2\pi} \sin^2\bar{n}\bar{x}_2\,\mathrm{d}\bar{x}_2 = \begin{cases} 0, & \text{when } \bar{n} = 0, \\ \pi, & \text{when } \bar{n} > 0, \end{cases} \tag{13}$$

$$\int_0^{2\pi} \cos^2\bar{n}\bar{x}_2\,\mathrm{d}\bar{x}_2 = \begin{cases} 2\pi, & \text{when } \bar{n} = 0, \\ \pi, & \text{when } \bar{n} > 0. \end{cases} \tag{14}$$

2.2. Ritz displacement functions

In order to apply the Ritz method, it is essential that the assumed displacement functions satisfy the geometric boundary conditions of the plate. The inner and outer peripheries of the annular plate are uniquely characterized by basic radial functions $\phi^\alpha_1(\bar{x}_1)$ in each of the displacement amplitude functions. The general form of this function is

$$\phi^\alpha_1(\bar{x}_1) = (\bar{x}_1 - \zeta)^{\Omega^\alpha_1}(\bar{x}_1 - 1)^{\Omega^\alpha_2}, \tag{15}$$

where $\zeta = r_\mathrm{i}/r_\mathrm{o}$ (inner-to-outer radius ratio).

The appropriate values for assigning to $\Omega^\alpha_\oplus$ for different boundary conditions are given as follows:

(a) *Free edge* (F): $\Omega^1_\oplus = \Omega^2_\oplus = \Omega^3_\oplus = 0$;

(b) *Soft simple support* (S*): $\Omega^1_\oplus = \Omega^2_\oplus = 0,\ \Omega^3_\oplus = 1$;

(c) *Hard simple support* (S): $\Omega^1_\oplus = 0,\ \Omega^2_\oplus = \Omega^3_\oplus = 1$;

(d) *Clamped edge* (C): $\Omega^1_\oplus = \Omega^2_\oplus = \Omega^3_\oplus = 1$

in which $\oplus = 1$, denotes the inner edge and $\oplus = 2$ the outer edge.

For the antisymmetric thickness modes, the basic functions $\psi_1^{\alpha}(\bar{x}_3)$ are

$$\psi_1^1(\bar{x}_3) = \bar{x}_3, \quad \psi_1^2(\bar{x}_3) = \bar{x}_3, \quad \psi_1^3(\bar{x}_3) = 1, \tag{16}$$

and for the symmetric thickness modes, the basic functions $\psi_1^{\alpha}(\bar{x}_3)$ take on the following values:

$$\psi_1^1(\bar{x}_3) = 1, \quad \psi_1^2(\bar{x}_3) = 1, \quad \psi_1^3(\bar{x}_3) = \bar{x}_3. \tag{17}$$

These sets of thickness variation functions satisfy the stress free requirement at the top and bottom surfaces of the plate at each thickness symmetry mode.

The higher-order polynomial functions for both radial functions $\phi_k^{\oplus}(\bar{x}_1)$ and thickness functions $\psi_k^{\oplus}(\bar{x}_3)$ are constructed according to a recurrence formula. For $P_k(x) \in \{\phi_k^{\oplus}, \psi_k^{\oplus};\ \oplus = 1, 2, 3\}$, the recurrence process gives

$$P_{k+1}(x) = \{g(x) - \Theta_k^A\}P_k(x) - \Theta_k^B P_{k-1}(x), \quad k = 1,\ 2,\ 3, \ldots, \tag{18}$$

where

$$g(x) = \begin{cases} \bar{x}_1, & \text{if } x = \bar{x}_1, \\ \bar{x}_3, & \text{if } x = \bar{x}_3. \end{cases} \tag{19}$$

In Eq. (18), the polynomial $P_0(x)$ is defined as zero, and the constants Θ_k^A and Θ_k^B are defined such that the set of polynomials generated maintain the orthogonality property:

$$\int_0^L P_j(x)P_k(x)\,\mathrm{d}x = \delta_{jk} \tag{20}$$

in which δ_{jk} is the Kronecker delta.

From the recurrence relation of Eq. (18) and considering Eq. (20), we have

$$\Theta_k^A = \frac{{}_3\Delta_k}{{}_4\Delta_k}, \tag{21}$$

$$\Theta_k^B = \frac{{}_4\Delta_k}{{}_5\Delta_{k-1}} \tag{22}$$

with

$${}_3\Delta_k = \int_0^L g(x)P_k^2(x)\,\mathrm{d}x, \tag{23}$$

$${}_4\Delta_k = \int_0^L P_k^2(x)\,\mathrm{d}x, \tag{24}$$

$${}_5\Delta_{k-1} = \int_0^L P_{k-1}^2(x)\,\mathrm{d}x. \tag{25}$$

2.3. Formation of the eigenvalue matrix

Let $\boldsymbol{\Pi}$ be the energy functional given by

$$\boldsymbol{\Pi} = \boldsymbol{V}_{\max} - \boldsymbol{T}_{\max}, \tag{26}$$

where $\boldsymbol{V}_{\max}$ and $\boldsymbol{T}_{\max}$ are the maximum strain and kinetic energies of a plate which are derived by substituting Eq. (9) into the respective energy expressions (1) and (8) with the periodic component $e^{i\omega t}$ eliminated.

The minimization of the functional in Eq. (26) with respect to the coefficients

$$\frac{\partial \boldsymbol{\Pi}}{\partial C^{\alpha}_{mn}} = 0, \quad \alpha = 1,\ 2,\ 3 \tag{27}$$

leading to the governing eigenvalue equation of the form

$$(\mathbf{K} - \hat{\lambda}^2\mathbf{M})\mathbf{C} = \mathbf{0}, \tag{28}$$

where

$$\mathbf{K} = \begin{bmatrix} \mathbf{k}^{11} & \mathbf{k}^{12} & \mathbf{k}^{13} \\ & \mathbf{k}^{22} & \mathbf{k}^{23} \\ \text{sym} & & \mathbf{k}^{33} \end{bmatrix}, \tag{29}$$

$$\mathbf{M} = \begin{bmatrix} \mathbf{m}^{11} & 0 & 0 \\ & \mathbf{m}^{22} & 0 \\ \text{sym} & & \mathbf{m}^{33} \end{bmatrix}, \tag{30}$$

$$\mathbf{C} = \begin{Bmatrix} \mathbf{C}^1 \\ \mathbf{C}^2 \\ \mathbf{C}^3 \end{Bmatrix}, \tag{31}$$

and $\hat{\lambda} = \omega r_{\mathrm{o}}\sqrt{\rho/E}$.

The explicit form of the respective elements in the stiffness submatrices $\mathbf{k}^{\alpha\beta}$ are given by:

$$\begin{aligned}\mathbf{k}^{11}_{mjnk} = {} & \frac{(1-\nu)S_1}{\boldsymbol{\Lambda}_1}\left\{\int_{\zeta}^{1}\bar{x}_1\frac{\mathrm{d}\phi^1_m}{\mathrm{d}\bar{x}_1}\frac{\mathrm{d}\phi^1_j}{\mathrm{d}\bar{x}_1}d\bar{x}_1 + \int_{\zeta}^{1}\bar{x}_1^{-1}\phi^1_m\phi^1_j\,\mathrm{d}\bar{x}_1\right\}\left(\Re^{00}_{nk}\right)_{11} \\ & + \frac{\nu S_1}{\boldsymbol{\Lambda}_1}\left\{\int_{\zeta}^{1}\phi^1_m\frac{\mathrm{d}\phi^1_j}{\mathrm{d}\bar{x}_1}\mathrm{d}\bar{x}_1 + \int_{\zeta}^{1}\frac{\mathrm{d}\phi^1_m}{\mathrm{d}\bar{x}_1}\phi^1_j\,\mathrm{d}\bar{x}_1\right\}\left(\Re^{00}_{nk}\right)_{11} \\ & + \frac{1}{\boldsymbol{\Lambda}_2}\left\{S_1\left(\int_{\zeta}^{1}\bar{x}_1\phi^1_m\phi^1_j\,\mathrm{d}\bar{x}_1\right)\left(\Re^{11}_{nk}\right)_{11} + S_2\bar{n}^2\left(\int_{\zeta}^{1}\bar{x}_1^{-1}\phi^1_m\phi^1_j\,\mathrm{d}\bar{x}_1\right)\left(\Re^{00}_{nk}\right)_{11}\right\},\end{aligned} \tag{32}$$

$$\begin{aligned}\mathbf{k}^{12}_{mjnk} = {} & \frac{(1-\nu)S_1\bar{n}}{\boldsymbol{\Lambda}_1}\left\{\int_{\zeta}^{1}\bar{x}_1^{-1}\phi^1_m\phi^2_j\,\mathrm{d}\bar{x}_1 + \frac{(1-2\nu)}{(1-\nu)}\int_{\zeta}^{1}\phi^1_m\frac{\mathrm{d}\phi^2_j}{\mathrm{d}\bar{x}_1}\mathrm{d}\bar{x}_1\right\}\left(\Re^{00}_{nk}\right)_{12} \\ & + \frac{S_2\bar{n}}{\boldsymbol{\Lambda}_2}\left\{\int_{\zeta}^{1}\bar{x}_1^{-1}\phi^1_m\phi^2_j\,\mathrm{d}\bar{x}_1 - \int_{\zeta}^{1}\frac{\mathrm{d}\phi^1_m}{\mathrm{d}\bar{x}_1}\phi^2_j\,\mathrm{d}\bar{x}_1\right\}\left(\Re^{00}_{nk}\right)_{12},\end{aligned} \tag{33}$$

$$\mathbf{k}^{13}_{mjnk} = \frac{S_1}{\boldsymbol{\Lambda}_1}\left\{\int_{\zeta}^{1}\bar{x}_1\frac{\mathrm{d}\phi^1_m}{\mathrm{d}\bar{x}_1}\phi^3_j\,\mathrm{d}\bar{x}_1 + \int_{\zeta}^{1}\phi^1_m\phi^3_j\,\mathrm{d}\bar{x}_1\right\}\left(\Re^{01}_{nk}\right)_{13} + \frac{S_1}{\boldsymbol{\Lambda}_2}\left\{\int_{\zeta}^{1}\bar{x}_1\phi^1_m\frac{\mathrm{d}\phi^3_j}{\mathrm{d}\bar{x}_1}\mathrm{d}\bar{x}_1\right\}\left(\Re^{10}_{nk}\right)_{13}, \tag{34}$$

$$\begin{aligned}\mathbf{k}^{22}_{mjnk} = {} & \frac{(1-\nu)S_1\bar{n}^2}{\boldsymbol{\Lambda}_1}\left\{\int_{\zeta}^{1}\bar{x}_1^{-1}\phi^2_m\phi^2_j\,\mathrm{d}\bar{x}_1\right\}(\Re^{00}_{nk})_{22} \\ & + \frac{S_2}{\boldsymbol{\Lambda}_2}\left\{\int_{\zeta}^{1}\bar{x}_1^{-1}\phi^2_m\phi^2_j\,\mathrm{d}\bar{x}_1 - \int_{\zeta}^{1}\frac{\mathrm{d}\phi^2_m}{\mathrm{d}\bar{x}_1}\phi^2_j\,\mathrm{d}\bar{x}_1\right\}(\Re^{00}_{nk})_{22} \\ & - \frac{S_2}{\boldsymbol{\Lambda}_2}\left\{\int_{\zeta}^{1}\phi^2_m\frac{\mathrm{d}\phi^2_j}{\mathrm{d}\bar{x}_1}\mathrm{d}\bar{x}_1 + \int_{\zeta}^{1}\bar{x}_1\frac{\mathrm{d}\phi^2_m}{\mathrm{d}\bar{x}_1}\frac{\mathrm{d}\phi^2_j}{\mathrm{d}\bar{x}_1}\mathrm{d}\bar{x}_1\right\}(\Re^{00}_{nk})_{22} + \frac{S_2}{\boldsymbol{\Lambda}_2}\left\{\int_{\zeta}^{1}\bar{x}_1\phi^2_m\phi^2_j\,\mathrm{d}\bar{x}_1\right\}\left(\Re^{11}_{nk}\right)_{22},\end{aligned} \tag{35}$$

$$\mathbf{k}^{23}_{mjnk} = \frac{S_1 \bar{n}}{\Lambda_1} \left\{ \int_\zeta^1 \phi^2_m \phi^3_j \, \mathrm{d}\bar{x}_1 \right\} (\Re^{01}_{nk})_{23} - \frac{S_2 \bar{n}}{\Lambda_2} \left\{ \int_\zeta^1 \phi^2_m \phi^3_j \, \mathrm{d}\bar{x}_1 \right\} (\Re^{10}_{nk})_{23}, \tag{36}$$

$$\begin{aligned} \mathbf{k}^{33}_{mjnk} = {} & \frac{(1-v)S_1}{\Lambda_1} \left\{ \int_\zeta^1 \bar{x}_1 \phi^3_m \phi^3_j \, \mathrm{d}\bar{x}_1 \right\} (\Re^{11}_{nk})_{33} \\ & + \frac{1}{\Lambda_2} \left\{ S_1 \int_\zeta^1 \bar{x}_1 \phi^3_m \phi^3_j \, \mathrm{d}\bar{x}_1 + S_2 \bar{n}^2 \int_\zeta^1 \bar{x}_1^{-1} \phi^3_m \phi^3_j \, \mathrm{d}\bar{x}_1 \right\} (\Re^{00}_{nk})_{33} \end{aligned} \tag{37}$$

and the elements in the mass submatrices $\mathbf{m}^{\alpha\beta}$ are given by

$$\mathbf{m}^{11}_{mjnk} = S_1 \left(\int_\zeta^1 \bar{x}_1 \phi^1_m \phi^1_j \, \mathrm{d}\bar{x}_1 \right) (\Re^{00}_{nk})_{11}, \tag{38}$$

$$\mathbf{m}^{22}_{mjnk} = S_1 \left(\int_\zeta^1 \bar{x}_1 \phi^2_m \phi^2_j \, \mathrm{d}\bar{x}_1 \right) (\Re^{00}_{nk})_{22}, \tag{39}$$

$$\mathbf{m}^{33}_{mjnk} = S_1 \left(\int_\zeta^1 \bar{x}_1 \phi^3_m \phi^3_j \, \mathrm{d}\bar{x}_1 \right) (\Re^{00}_{nk})_{33}, \tag{40}$$

where

$$\Lambda_1 = (1-2v)\Lambda_2, \tag{41}$$

$$\Lambda_2 = (1+v), \tag{42}$$

$$(\Re^{rs}_{nk})_{\alpha\beta} = \int_{-1/2}^{1/2} \frac{\partial^r \psi^\alpha_n(\bar{x}_3)}{\partial \bar{x}_3^r} \frac{\partial^s \psi^\beta_k(\bar{x}_3)}{\partial \bar{x}_3^s} \, \mathrm{d}\bar{x}_3 \tag{43}$$

in which

$$\langle \alpha; \beta \rangle = \langle 1,2,3;\ 1,2,3 \rangle. \tag{44}$$

The scalars S_1 and S_2 are defined as

$$S_1 = \begin{cases} 2 & \text{when } \bar{n} = 0, \\ 1 & \text{when } \bar{n} > 0, \end{cases} \tag{45}$$

and

$$S_2 = \begin{cases} 0 & \text{when } \bar{n} = 0, \\ 1 & \text{when } \bar{n} > 0. \end{cases} \tag{46}$$

To be consistent with the frequency parameter generally defined in the literature, the eigenvalue in Eq. (28) is nondimensionalized to the following form:

$$\lambda = \frac{\omega r_\mathrm{o}^2}{2\pi} \sqrt{\frac{\rho h}{D}}, \tag{47}$$

where D is the flexural rigidity of the plate.

For the special case in which the mode shape does not possess any nodal diameter ($\bar{n} = 0$), the eigenvalue equation can be reduced to the following form which governs only the axisymmetric ($\bar{n} = 0$) vibration modes of the plate

Table 1
Convergence of the first eight frequency parameters for annular plates with different boundary conditions ($r_i/r_o = 0.30$ and $h/r_o = 0.20$)

Terms	Mode sequence number $(\bar{n}, \bar{s})$							
$M \times N$	1	2	3	4	5	6	7	8
(a) An annular plate with hard simply supported outer edge and free inner edge (S–F)								
5 × 4	4.5427 (0,0)	11.250 (1,0)	12.750 (1,0)[a]	15.936 (2,0)[a]	20.854 (2,0)	27.942 (0,0)[a]	30.774 (0,1)	31.549 (3,0)
5 × 5	4.5427 (0,0)	11.250 (1,0)	12.750 (1,0)[a]	15.936 (2,0)[a]	20.854 (2,0)	27.942 (0,0)[a]	30.774 (0,1)	31.549 (3,0)
6 × 4	4.5408 (0,0)	11.243 (1,0)	12.745 (1,0)[a]	15.918 (2,0)[a]	20.853 (2,0)	27.933 (0,0)[a]	30.710 (0,1)	31.544 (3,0)
7 × 4	4.5405 (0,0)	11.240 (1,0)	12.743 (1,0)[a]	15.907 (2,0)[a]	20.852 (2,0)	27.932 (0,0)[a]	30.709 (0,1)	31.543 (3,0)
8 × 4	4.5402 (0,0)	11.240 (1,0)	12.742 (1,0)[a]	15.905 (2,0)[a]	20.852 (2,0)	27.931 (0,0)[a]	30.709 (0,1)	31.543 (3,0)
9 × 4	4.5401 (0,0)	11.240 (1,0)	12.742 (1,0)[a]	15.904 (2,0)[a]	20.852 (2,0)	27.931 (0,0)[a]	30.709 (0,1)	31.543 (3,0)
(b) An annular plate with both outer and inner edges free (F–F)								
5 × 4	4.6360 (2,0)	7.8983 (0,1)	11.170 (3,0)	15.279 (1,1)	15.711 (2,0)[a]	18.862 (4,0)	26.895 (2,1)	27.429 (5,0)
5 × 5	4.6360 (2,0)	7.8983 (0,1)	11.170 (3,0)	15.279 (1,1)	15.711 (2,0)[a]	18.862 (4,0)	26.895 (2,1)	27.429 (5,0)
6 × 4	4.6219 (2,0)	7.8942 (0,1)	11.146 (3,0)	15.201 (1,1)	15.673 (2,0)[a]	18.830 (4,0)	26.814 (2,1)	27.387 (5,0)
7 × 4	4.6208 (2,0)	7.8939 (0,1)	11.145 (3,0)	15.192 (1,1)	15.664 (2,0)[a]	18.828 (4,0)	26.812 (2,1)	27.380 (5,0)
8 × 4	4.6200 (2,0)	7.8939 (0,1)	11.144 (3,0)	15.189 (1,1)	15.662 (2,0)[a]	18.826 (4,0)	26.810 (2,1)	27.378 (5,0)
9 × 4	4.6198 (2,0)	7.8939 (0,1)	11.143 (3,0)	15.189 (1,1)	15.662 (2,0)[a]	18.826 (4,0)	26.810 (2,1)	27.378 (5,0)
(c) An annular plate with clamped outer edge and free inner edge (C–F)								
5 × 4	10.480 (0,0)	16.072 (1,0)	25.699 (2,0)	36.278 (3,0)	37.441 (0,1)	39.635 (1,0)[a]	40.939 (1,1)	44.118 (2,0)[a]
5 × 5	10.480 (0,0)	16.072 (1,0)	25.699 (2,0)	36.278 (3,0)	37.441 (0,1)	39.635 (1,0)[a]	40.939 (1,1)	44.118 (2,0)[a]
6 × 4	10.463 (0,0)	16.044 (1,0)	25.673 (2,0)	36.244 (3,0)	37.396 (0,1)	39.618 (1,0)[a]	40.854 (1,1)	44.099 (2,0)[a]
7 × 4	10.454 (0,0)	16.031 (1,0)	25.659 (2,0)	36.228 (3,0)	37.360 (0,1)	39.609 (1,0)[a]	40.827 (1,1)	44.086 (2,0)[a]
8 × 4	10.448 (0,0)	16.027 (1,0)	25.651 (2,0)	36.221 (3,0)	37.348 (0,1)	39.603 (1,0)[a]	40.810 (1,1)	44.080 (2,0)[a]
9 × 4	10.448 (0,0)	16.026 (1,0)	25.650 (2,0)	36.220 (3,0)	37.346 (0,1)	39.602 (1,0)[a]	40.809 (1,1)	44.080 (2,0)[a]

[a] Denotes symmetric thickness mode.

$$(\mathbf{K} - \hat{\lambda}^2\mathbf{M})\mathbf{C} = \mathbf{0}, \tag{48}$$

where

$$\mathbf{K} = \begin{bmatrix} \mathbf{k}^{11} & \mathbf{k}^{13} \\ \text{sym} & \mathbf{k}^{33} \end{bmatrix}, \tag{49}$$

$$\mathbf{M} = \begin{bmatrix} \mathbf{m}^{11} & \mathbf{0} \\ \text{sym} & \mathbf{m}^{33} \end{bmatrix}, \tag{50}$$

$$\mathbf{C} = \begin{Bmatrix} \mathbf{C}^1 \\ \mathbf{C}^3 \end{Bmatrix} \tag{51}$$

in which the terms in Eq. (51) are determined by setting $\bar{n} = 0$.

3. Results and discussion

The above procedure is applied to compute the natural frequencies and mode shapes of annular plates with various combinations of boundary conditions, relative thickness ratio h/r_o and cutout ratio r_i/r_o. Two example plate problems are considered: (a) an annular plate with a free inner edge but the outer edge is subjected to either a free, simply supported or clamped boundary condition, and (b) an annular plate with a restrained inner edge and where the outer edge is subjected to either a free, simply supported or clamped

Table 2
Comparison of frequency parameters for annular plates with free inner edge and various restrained outer edges (antisymmetric thickness modes)

h/r_o	r_i/r_o	Source of results	Mode types[a] (0,1)	(0,2)	(1,1)	(1,2)	(2,1)	(2,2)
(a) Annular plates with free inner and outer edges (F–F)								
0.10	0.10	FSDT[b]	8.65	35.95	19.56	52.90	5.21	32.69
		Authors	8.6518	36.036	19.596	53.148	5.2105	32.786
	0.30	FSDT[b]	8.23	46.63	17.02	52.50	4.80	30.77
		Authors	8.2291	46.73	17.063	52.693	4.7996	30.842
	0.50	FSDT[b]	9.10	81.03	15.76	83.48	4.17	28.05
		Authors	9.1036	81.306	15.783	83.770	4.1730	28.085
0.30	0.10	FSDT[b]	7.83	26.58	15.70	34.62	4.81	24.12
		Authors	7.8544	26.865	15.824	35.170	4.8172	24.403
	0.30	FSDT[b]	7.42	33.18	13.16	35.42	4.38	22.52
		Authors	7.4313	33.501	13.247	35.801	4.3921	22.758
	0.50	FSDT[b]	7.84	51.25	11.72	51.94	3.78	19.42
		Authors	7.8482	51.785	11.778	52.504	3.7900	19.567
(b) Annular plates with free inner and hard simply supported outer edges (S–F)								
0.10	0.10	FSDT[b]	4.81	28.04	13.50	43.83	24.26	61.94
		Authors	4.8181	28.104	13.524	44.016	24.316	62.271
	0.30	FSDT[b]	4.63	34.92	12.19	41.45	23.07	57.18
		Authors	4.6329	35.002	12.208	41.582	23.116	57.445
	0.50	FSDT[b]	5.03	59.53	10.90	62.28	20.92	70.09
		Authors	5.0352	59.721	10.916	62.503	20.966	70.510
0.30	0.10	FSDT[b]	4.54	21.67	11.50	30.05	19.04	39.93
		Authors	4.5572	21.933	11.602	30.565	19.279	40.757
	0.30	FSDT[b]	4.39	26.08	10.09	28.93	18.13	36.61
		Authors	4.4007	26.387	10.162	29.307	18.340	37.184
	0.50	FSDT[b]	4.72	39.22	8.94	40.24	16.11	43.25
		Authors	4.7367	39.798	8.9904	40.836	16.256	42.972
(c) Annular plates with free inner and clamped outer edges (C–F)								
0.10	0.10	FSDT[b]	9.90	36.33	20.04	52.53	31.86	71.35
		Authors	9.9490	36.603	20.171	53.015	32.095	72.083
	0.30	FSDT[b]	11.12	46.25	18.12	51.74	30.08	66.24
		Authors	11.180	46.641	18.220	52.173	30.266	66.828
	0.50	FSDT[b]	17.02	77.24	20.48	79.41	29.02	85.76
		Authors	17.142	78.150	20.614	80.339	29.197	86.748
0.30	0.10	FSDT[b]	8.37	24.70	15.01	32.23	22.02	41.64
		Authors	8.4771	25.203	15.274	32.982	22.461	42.734
	0.30	FSDT[b]	9.39	29.08	13.64	31.32	20.96	38.10
		Authors	9.5132	29.701	13.835	31.978	21.348	38.905
	0.50	FSDT[b]	13.55	40.90	15.42	41.71	20.21	44.29
		Authors	13.773	41.952	15.669	41.952	20.540	45.355

[a] The first number denotes the number of nodal diameters, whereas the second number indicates the order of the frequencies.
[b] Irie et al. (1982).

boundary condition. The following section presents the accuracy of the method by checking the convergence and comparing it with existing results and finite element solutions, followed by a parametric study. The first known vibration frequencies and mode shapes for selected annular plates are also presented for both cases.

Table 3
Comparison of frequency parameters with finite element solutions for annular plates subjected to S–F and C–F boundary conditions ($r_i/r_o = 0.30$ and $h/r_o = 0.20$)

Boundary condition	Source of results	Mode sequence number							
		1	2	3	4	5	6	7	8
S–F	FE method[a]	4.6848	11.881	–	–	21.133	–	30.804	31.364
	Authors	4.5402	11.240	12.742	15.905	20.852	27.931	30.709	31.543
C–F	FE method	10.440	16.085	25.723	36.174	37.136	39.479	–	–
	Authors	10.448	16.027	25.651	36.221	37.348	39.603	40.810	44.080

[a] Solutions obtained using eight-node 3-D element of MSC/NASTRAN software package with 3000 elements (3960 nodes).

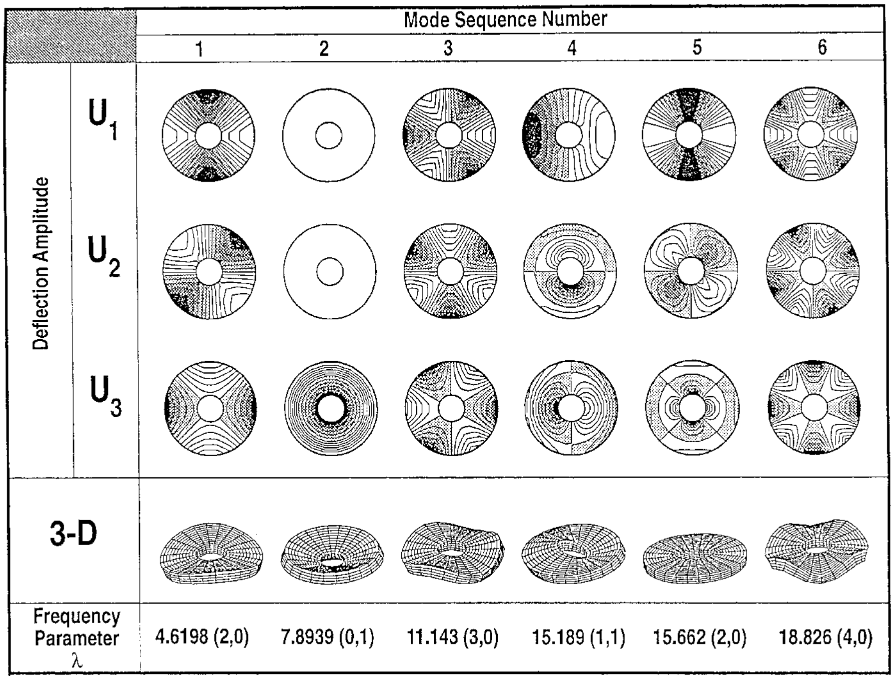

Fig. 2. Deformed mode shapes and frequency parameters of an annular plate with both the inner and outer edges free ($r_i/r_o = 0.30$, $h/r_o = 0.20$).

Table 1 shows the effects of different boundary conditions (at the inner and outer edges) on the rate of convergence of the frequency parameters. Annular plates with both outer and inner edges free (F–F), hard simply supported outer edge and free inner edge (S–F), and clamped outer edge and free inner edge (C–F) are considered. The number of terms assumed in each displacement component is stepped from 5×4 to 9×4 to illustrate the improvement in the frequency convergence. It is observed that as the number of terms of N is increased from 4 to 5, the rate of convergence does not increase. However when M increases, the solution converges to a better upper-bound value. Reasonably accurate frequency solutions for the first eight modes of vibration are achieved when 8×4 terms are used in the displacement functions.

In Table 2, a comparison study of the results for the annular plates with F–F, S–F, and C–F boundary conditions with the Mindlin solutions of Irie et al. (1982) is carried out. From this comparison, it is found that for small thickness ratio, $h/r_o = 0.10$, the three-dimensional frequency solutions and the Mindlin plate approximations are in good agreement for annular plates with a free or hard simply supported outer edge.

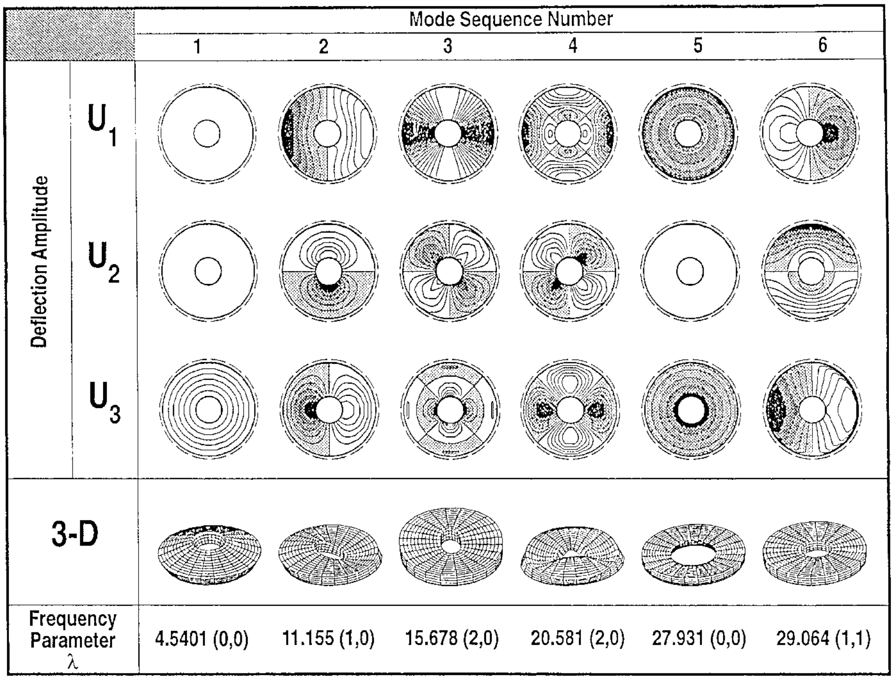

Fig. 3. Deformed mode shapes and frequency parameters of an annular plate with a soft simply supported outer edge and a free inner edge ($r_i/r_o = 0.30,\ h/r_o = 0.20$).

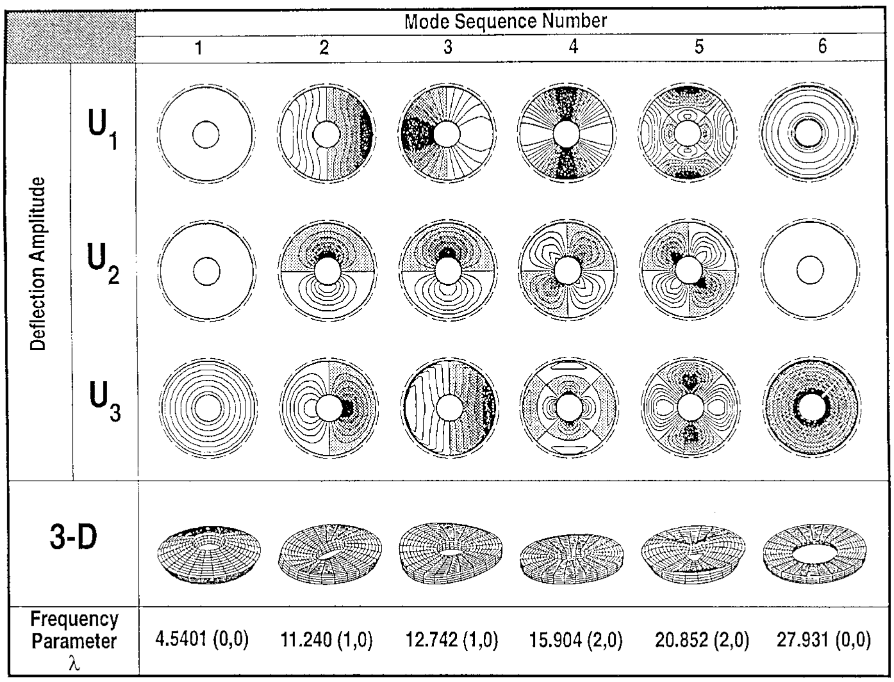

Fig. 4. Deformed mode shapes and frequency parameters of an annular plate with a hard simply supported outer edge and a free inner edge ($r_i/r_o = 0.30,\ h/r_o = 0.20$).

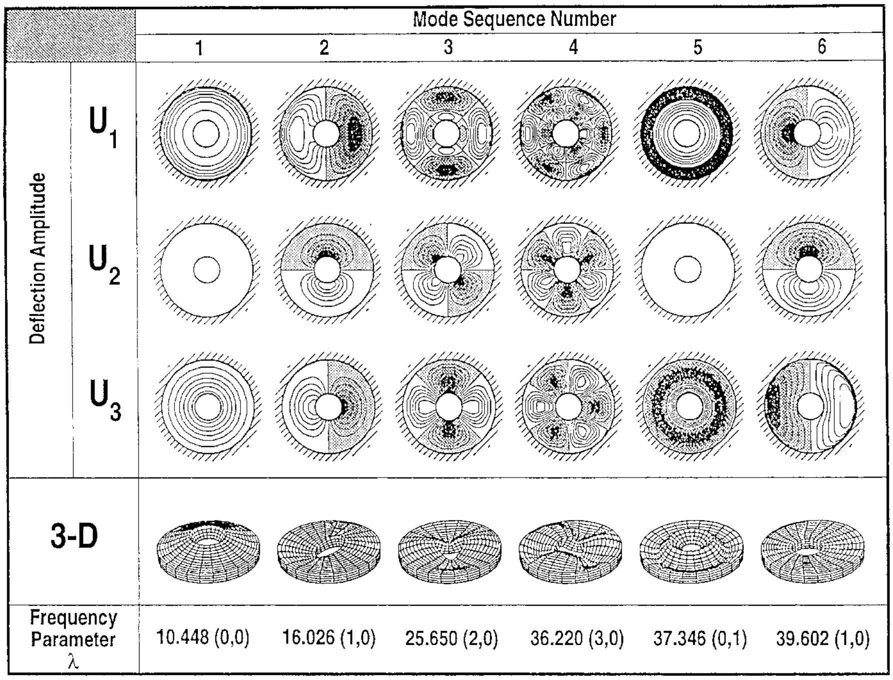

Fig. 5. Deformed mode shapes and frequency parameters of an annular plate with a clamped outer edge and a free inner edge ($r_i/r_o = 0.30,\ h/r_o = 0.20$).

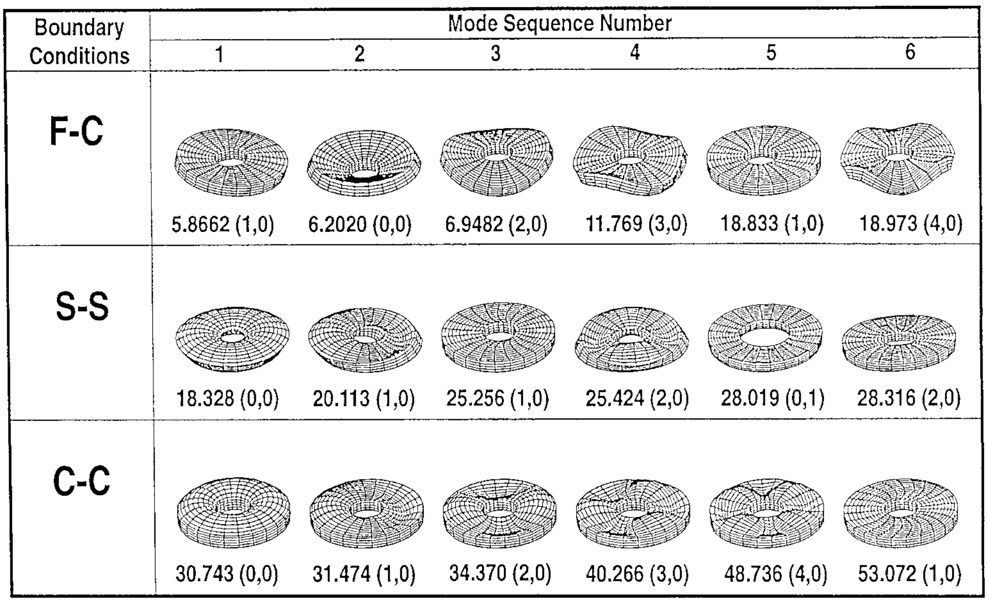

Fig. 6. Deformed mode shapes and frequency parameters of annular plates with F–C, S–S and C–C boundary conditions ($r_i/r_o = 0.30,\ h/r_o = 0.20$).

However, the discrepancy increases for annular plates with a clamped outer edge and particularly at higher relative thickness ratios, $h/r_o = 0.30$ and 0.50. This is attributed to the fact that the first-order Mindlin theory assumes linear variations across the thickness, which is only valid for plates with moderate thickness ratios, h/r_o. Table 3 shows a comparison study of the present results with the converged finite element solutions obtained using the MSC/NASTRAN software package. A good agreement is achieved between the present results and the finite element solutions.

The three-dimensional vibration mode shapes of the annular plates are shown in Figs. 2–5 for free, soft simply supported, hard simply supported and clamped outer edges. Displacement components in the radial (U_1), circumferential (U_2) and thickness (U_3) directions are presented together with the three-dimensional mode shape plots. It is observed that for the antisymmetric thickness modes, the index $\bar{n}$ correlates to the number of nodal diameters appearing in the out-of-plane (U_3) vibration modes. The second mode of the free annular plate is noted as an axisymmetric mode, and the fifth mode is a symmetric thickness mode with distinct stretching and contracting motions at the inner cutout. The fundamental modes for both the hard and soft simple supports have an identical frequency value ($\lambda = 4.5401$) and mode shape. An identical frequency value is also observed for the axisymmetry in-plane vibration mode ($\lambda = 27.931$).

The mode shapes of thick annular plates with F–C, S–S and C–C boundary conditions are depicted in Fig. 6. The plate thickness ratio h/r_o and cut-out ratio r_i/r_o are fixed at 0.20 and 0.30 for the purposed of generating these plots. Annular plates with free outer and clamped inner boundaries, comparatively have the lowest vibration frequencies. The fundamental mode, for this case, has a distinct nodal diameter. On the other hand, for both the hard simply supported and fully clamped annular plates, the fundamental modes are axisymmetric out-of-plane modes. It is also observed that the vibration spectrum of the hard, simply supported annular plate appears to possess the most number of thickness symmetric in-plane vibration modes.

4. Conclusions

Three-dimensional elasticity solutions for free vibrations of annular plates with various combinations of inner and outer boundary conditions were presented. A systematic formulation of the integral expressions for strain and kinetic energies in a cylindrical polar coordinate system was detailed. The linear small-strain three-dimensional elasticity theory adopted in this derivation allows computation of the full vibration spectrum for the plates. Following the Ritz procedure and with the use of a set of uniquely constructed orthogonal polynomials as the admissible functions, a linear eigenvalue equation system was obtained. This was used to determine the vibration frequencies and mode shapes of the plates. In the admissible functions, the orthogonality inherent in the polynomial series results in better computational efficiency. A monotonic convergence for this model was ensured.

After the validation of the present results with the available analytical solutions and also the finite element solutions that obtained using the MSC/NASTRAN software package for some problems in the literature, vibration behaviours of annular plates with various thickness ratios and different combinations of inner and outer boundary conditions were investigated. Vivid graphical representations of the vibration modes were manifested in shaded contour plots and three-dimensional deformed mesh geometry. The three-dimensional mode shapes encompass flexural, thickness twist and thickness shear motions, and in particular the twist and shear modes which cannot be predicted by the two-dimensional plate theories.

References

Deresiewicz, H., Mindlin, R.D., 1955. Axially symmetric flexural vibrations of a circular disk. Journal of Applied Mechanics 22, 86–88.
Irie, T., Yamada, G., Takagi, K., 1982. Natural frequencies of thick annular plates. Journal of Applied Mechanics 49, 633–638.

Kim, C.S., Dickinson, S.M., 1989. On the lateral vibration of thin annular and circular composite plates subject to certain complicating effects. Journal of Sound and Vibration 130, 363–377.

Leissa, A.W., 1969. Vibration of plates, NASA SP-169. Office of Technology Utilization, Washington, DC.

Liew, K.M., 1993. Treatments of over-restrained boundaries for doubly connected plates of arbitrary shape in vibration analysis. International Journal of Solids and Structures 30, 337–347.

Liew, K.M., Xiang, Y., Wang, C.M., Kitipornchai, S., 1993a. Flexural vibration of shear deformable circular and annular plates on ring supports. Computer Methods in Applied Mechanics and Engineering 110, 301–315.

Liew, K.M., Hung, K.C., Lim, M.K., 1993b. A continuum three-dimensional vibration analysis of thick rectangular plates. International Journal of Solids and Structures 30, 3357–3379.

Liew, K.M., Hung, K.C., 1995. Three-dimensional vibratory characteristics of solid cylinders and some remarks on simplified beam theories. International Journal of Solids and Structures 32, 3499–3513.

Liew, K.M., Xiang, Y., Kitipornchai, S., 1995a. Research on thick plate vibration: a literature survey. Journal of Sound and Vibration 180, 163–176.

Liew, K.M., Hung, K.C., Lim, M.K., 1995b. Vibration of stress-free hollow cylinders of arbitrary cross section. Journal of Applied Mechanics 62, 718–724.

Liew, K.M., Yang, B., 1999. Three-dimensional elasticity solutions for free vibrations of circular plates: a polynomials-Ritz analysis. Computer Methods in Applied Mechanics and Engineering 175, 189–201.

Nosier, A., Kapania, R.K., Reddy, J.N., 1993. Free vibration analysis of laminated plates using a layerwise theory. AIAA Journal 31, 2335–2346.

Srinivas, S., Rao, A.K., 1970. Bending, vibration and buckling of simply supported thick orthotropic rectangular plates and laminates. International Journal of Solids and Structures 6, 1463–1481.